

<https://doi.org/10.1038/s41612-025-01124-7>

# Co-drivers of air pollutant and CO<sub>2</sub> emissions in China from 2000 to 2020



Wenxin Cao<sup>1,2,3,4</sup>, Yixuan Zheng<sup>2</sup>✉, Shaohui Zhang<sup>5</sup>, Zbigniew Klimont<sup>5</sup>, Xian'en Wang<sup>1,3,4</sup>✉, Fangming Jiang<sup>6</sup>, Zhulin Qi<sup>6</sup>, Chuchu Chen<sup>7</sup>, Yueyi Feng<sup>2</sup>, Zechen Zhang<sup>2</sup>, Hongkuan Zang<sup>7,8</sup>, Yu Lei<sup>2</sup> & Gang Yan<sup>2</sup>✉

Revealing how historical energy and environmental policies interacted with socioeconomic factors to shape the trends in air pollutant and CO<sub>2</sub> emissions is crucial for developing effective future pollution-carbon co-control strategies. Here, we develop an integrated analytical framework combining a detailed sectoral emission inventory, index decomposition analysis, and a clustering algorithm to investigate China's synergetic patterns of air pollutant and CO<sub>2</sub> emissions across 15 socioeconomic sectors from 2000 to 2020 and uncover the co-drivers behind these trends, with detailed temporal, sectoral, and spatial dynamics revealed. Our analysis suggests that historical policies have effectively curbed air pollutant emissions, while abating CO<sub>2</sub> emissions remains a challenge. Energy and climate policies, particularly those focused on structural adjustments, are increasingly instrumental in driving pollution-carbon co-reduction. Compared to the earlier period, the fractional contribution of energy and climate policies to emission reductions of SO<sub>2</sub>, NO<sub>x</sub>, PM<sub>2.5</sub>, and CO<sub>2</sub> increased by 1.3–8.6 times during 2010–2020, respectively. Substantial regional heterogeneity in emission co-drivers underscores the need for tailored strategies, such as adopting advanced energy-saving technologies in areas dominated by energy-intensive industries and accelerating the clean energy transition in regions endowed with renewable resources. Our study would provide actionable insights for formulating effective pollution-carbon co-control strategies in China and beyond.

Over the past few decades, China's swift economic expansion has led to substantial deteriorations in air quality and associated public health, as well as a surge in CO<sub>2</sub> emissions, primarily driven by energy-intensive and coal-dependent industries<sup>1–3</sup>. As reported by the Ministry of Ecology and Environment of China (MEE), the national annual average PM<sub>2.5</sub> concentration was 29.3 μg m<sup>-3</sup> in 2024<sup>4</sup>, still far exceeding the air quality guideline suggested by the World Health Organization (that is, annual average PM<sub>2.5</sub> concentration less than 5 μg m<sup>-3</sup>). Furthermore, as the largest contributor to global CO<sub>2</sub> emissions, China may have experienced a 5.2% increase in CO<sub>2</sub> emissions from energy consumption from 2022 to 2023<sup>5</sup>. In response to the intertwined issues of air pollution and climate change, the government of China introduced the “Implementation Plan for Synergizing Reduction of Pollution and Carbon Emission” in 2022. Guided by the

theoretical foundation that emissions of air pollutants and CO<sub>2</sub> are mainly rooted in the “same sources” or the “same processes”, it prioritizes energy structural adjustments and the optimization of industrial layouts to attain pollution-carbon co-control. Measures including transitioning to renewable energy sources and eliminating outdated production capacities can deliver notable co-benefits in mitigating air pollution and curbing the growth of CO<sub>2</sub> emissions<sup>6–8</sup>.

Despite air pollutants and CO<sub>2</sub> are characterized by sharing a common origin in general, sectoral and regional contributions may vary greatly by species<sup>9</sup>. Moreover, environmental impacts of CO<sub>2</sub> emissions from various emission sources tend to be homogeneous, whereas impacts caused by air pollutant emissions are highly correlated with source locations and sectors, thereby leading to disparities in policy effectiveness. In pursuit of cleaner air

<sup>1</sup>College of New Energy and Environment, Jilin University, Changchun, China. <sup>2</sup>Key Laboratory of Environmental Pollution and Greenhouse Gases Co-control, Ministry of Ecology and Environment, Chinese Academy of Environmental Planning, Beijing, China. <sup>3</sup>Jilin Provincial Key Laboratory of Water Resources and Environment, Jilin University, Changchun, China. <sup>4</sup>Key Laboratory of Groundwater Resources and Environment, Ministry of Education, Jilin University, Changchun, China. <sup>5</sup>International Institute for Applied Systems Analysis, Laxenburg, Austria. <sup>6</sup>College of Environmental & Resource Sciences, Zhejiang University, Hangzhou, China. <sup>7</sup>State Key Joint Laboratory of Environmental Simulation and Pollution Control, School of Environment, Tsinghua University, Beijing, China. <sup>8</sup>Beijing Enterprises Water Group Limited, Beijing, China. ✉e-mail: [zhengyx@caep.org.cn](mailto:zhengyx@caep.org.cn); [wxen@jlu.edu.cn](mailto:wxen@jlu.edu.cn); [yangang@caep.org.cn](mailto:yangang@caep.org.cn)

and low-carbon emission goals, the country has enacted a series of energy, climate, and environmental policies, such as implementing the “ultra-low” emission renovation in the power and industrial sectors, retiring yellow-label and old vehicles (i.e., old and high-emission vehicles that fail to meet given exhaust emission standards), and promoting clean energy transition in the residential sector<sup>10–12</sup>. Driven by distinct policy focus, the effectiveness of these policies in shaping air pollutant and CO<sub>2</sub> emission patterns is anticipated to differ greatly, depending on whether the priority is given to pollution control, carbon reduction, or pollution-carbon co-control; while some may facilitate synergies, others could lead to trade-offs<sup>13–15</sup>. Additionally, the effects of implemented policies may vary due to their interactions with China’s evolving socioeconomic development trajectory, as energy and production demands are key drivers determining generations of air pollutant and CO<sub>2</sub> emissions<sup>16</sup>. Therefore, in the context of pollution-carbon co-control, uncovering the spatial and sectoral heterogeneity in the impacts of historical policy interventions and socioeconomic factors on air pollutant and CO<sub>2</sub> emissions is crucial for guiding the design of future co-control strategies.

Regarding the interaction of clean air actions or decarbonization efforts, previous studies have extensively demonstrated the substantial co-benefits of these policies that are proposed from distinct original purposes<sup>17–20</sup>. However, the synergies or trade-offs between air pollutant and CO<sub>2</sub> emissions, shaped by long-term policy portfolios, remain unclear. Studies have been conducted to quantify the impacts of various socioeconomic and policy factors on changes in energy consumption, air pollutant emissions, and air quality improvement, as well as CO<sub>2</sub> emissions<sup>21–25</sup>. However, these studies typically focus on a single carbon or air pollutant dimension. Although several attempts have been made to identify drivers that synergistically drove changes in air pollutant and CO<sub>2</sub> emissions, most are limited to relatively narrow and lagged periods (e.g., 2005–2015)<sup>26,27</sup>. Recent research has extended the temporal coverage to uncover provincial-level drivers of synergetic efficiency, however, sectoral heterogeneity remains poorly understood<sup>16</sup>. Additionally, existing sector-specific investigations of co-drivers mainly focused on key sectors (e.g., power and transportation)<sup>28–30</sup>, fail to systematically reveal the cross-sectoral co-driving mechanisms behind emission trends. Despite regional emission mitigation pathways have been initially explored with sectoral information incorporated, regional divisions often rely on economic levels or geographical locations, which may overlook the interplay among emission dynamics, local socioeconomic development, and region-specific policy interventions<sup>31,32</sup>. Hence, a comprehensive assessment that integrates detailed spatial and sectoral information to identify co-drivers of air pollutant and CO<sub>2</sub> emissions over a long-term period is still lacking. Addressing such a question would reveal the underlying spatial heterogeneity behind these drivers, thereby providing key insights to inform the formulation of region-specific co-control strategies in the future.

Here, we comprehensively explore the heterogeneity in co-drivers of air pollutant and CO<sub>2</sub> emissions across detailed spatial and sectoral sources (i.e., 15 sectors from 30 provinces) during 2000–2020 for the first time, and identify the characteristics of pollution-carbon co-control across different provincial types in China. First, a detailed sector-specific inventory of air pollutant and CO<sub>2</sub> emissions from 2000 to 2020, with five-year intervals, is derived and updated based on the Greenhouse Gas-Air Pollution Interactions and Synergies model adapted to China (GAINS-China). We further analyze the synergetic patterns based on sectoral air pollutant and CO<sub>2</sub> emission trends. Then, we apply an index decomposition method to identify the co-drivers behind air pollutant and CO<sub>2</sub> emission trends. This involves decomposing the effects of different socioeconomic and policy factors on emission changes, as demonstrated in the emission inventory over a long period across China. Finally, on the basis of aggregating the effects of drivers on emission trends across different provinces, a clustering analysis approach is further employed to group 30 provinces (excluding Tibet, Hong Kong, Macao, and Taiwan due to data availability), enabling the identification of spatially distinct pollution-carbon co-control characteristics. Tailored policy recommendations to guide the development of region-specific co-control strategies are then proposed.

## Results

### Trends in China’s air pollutant and CO<sub>2</sub> emissions from 2000 to 2020

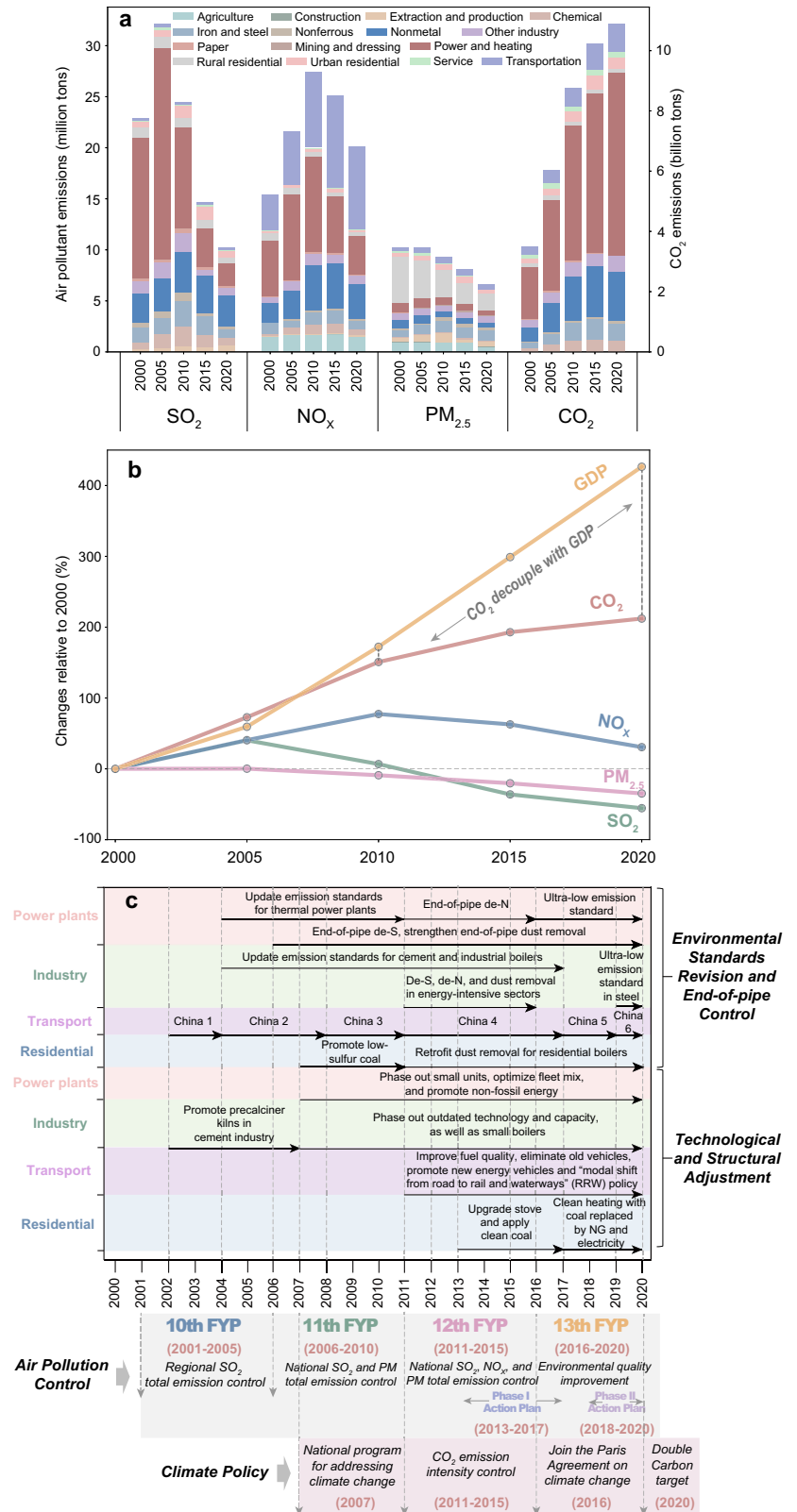
Figure 1 shows emission patterns of three major air pollutants (that is, SO<sub>2</sub>, NO<sub>x</sub>, primary PM<sub>2.5</sub>), and CO<sub>2</sub> across China during 2000–2020. Notably, due to the 5-year interval settings in the GAINS-China model, our analysis of emission trends captures multi-year patterns that might fail to capture the exact peak year for specific air pollutant emissions. Between 2000 and 2020, emissions of SO<sub>2</sub> and primary PM<sub>2.5</sub> declined by 55.5% and 34.8%, respectively, while NO<sub>x</sub> emissions increased by 30.6%. The stage-based emission patterns observed over the past two decades are consistent with findings documented in other inventories (Supplementary Fig. S1). All three major air pollutant emissions have followed a downward trajectory since 2010. From 2005 to 2020, emissions of SO<sub>2</sub> and primary PM<sub>2.5</sub> exhibited continuous declines of 68.3% and 34.9%, respectively, demonstrating the effectiveness of implementing total emission control of SO<sub>2</sub> and particulate matter in the 11<sup>th</sup> Five Year Plan (FYP; i.e., the 11<sup>th</sup> FYP period covers 2006–2010)<sup>33</sup>. The NO<sub>x</sub> emission profile showed relatively different, with an upward trend of 26.2% between 2005 and 2010, followed by a 26.4% decrease from 2010 to 2020. This noted disparity can be explained by the delay in introducing total NO<sub>x</sub> emission control policy, which was not implemented until the 12<sup>th</sup> FYP (i.e., the 12<sup>th</sup> FYP period covers 2011–2015)<sup>34</sup>. Different sectoral sources contribute to divergences in the emission structure of various air pollutants over time. The power and heating sector demonstrated the major contributor to SO<sub>2</sub> and NO<sub>x</sub> emissions before 2010, accounting for 40.6% and 34% of national SO<sub>2</sub> and NO<sub>x</sub> emissions in 2010, respectively, driven by the rapid increase in sectoral electricity generation<sup>35</sup>. From 2015 to 2020, the nonmetal sector gradually emerged as a key source of SO<sub>2</sub> emissions, responsible for 30.6% of the national total in 2020, while the transportation sector led national NO<sub>x</sub> emissions (40.4% of the total in 2020). This shift was largely attributed to substantial reductions in SO<sub>2</sub> and NO<sub>x</sub> emissions from the power and heating sector. Over the past two decades, the rural residential sector has remained the dominant contributor to national primary PM<sub>2.5</sub> emissions, contributing about a quarter of the national total in 2020. Notably, emissions of NO<sub>x</sub> and PM<sub>2.5</sub> in the agriculture sector were mainly sourced from manure application on small farms and agricultural waste burning, respectively.

In contrast to the decreasing patterns in air pollutant emissions, China’s total CO<sub>2</sub> emissions followed a continuously upward trajectory, but with a slower growth rate. During 2000–2020, national CO<sub>2</sub> emissions were estimated to increase by 212.1% to 10.9 billion tons, with an average annual rate of 10.6%. As shown in Fig. 1b, a notable downturn in the annual growth rate of CO<sub>2</sub> emissions has occurred since 2010, due to the implementation of carbon emission intensity controls under the 12<sup>th</sup> FYP period<sup>34</sup>. Specifically, national CO<sub>2</sub> emissions grew by only 24.5% from 2010 to 2020, while GDP surged by 93.3%, despite being impacted by the contraction of industrial and socioeconomic activities during the COVID-19 lockdown in 2020. This indicates that China’s CO<sub>2</sub> emissions have shown a relatively decoupled pattern from economic growth since 2010. Additionally, identified key sources of air pollutant emissions, that is, the power and heating, nonmetal, and transportation sectors, also contributed substantially to the increase in national CO<sub>2</sub> emissions during the whole period. For example, the power and heating sector was estimated to contribute 58.5% to the total change in CO<sub>2</sub> emissions from 2000 to 2020, which can be largely attributed to the ongoing growth in fossil fuel consumption, particularly with the share of coal consumption reaching 70.5% in the power and heating sector in 2020 (Supplementary Fig. S2).

### Synergies in air pollutant and CO<sub>2</sub> emissions across key sectors

Figure 2 illustrates the synergetic relationships between air pollutant and CO<sub>2</sub> emissions across six key sectors (i.e., the iron and steel, nonmetal, nonferrous metal, power and heating, transportation, and rural residential sectors), based on their temporal evolving trends from 2000 to 2020. These six key sectors were estimated to account for 66.8–83.2% of national air pollutant emissions and 86.3% of total CO<sub>2</sub> emissions in 2020. Over the past

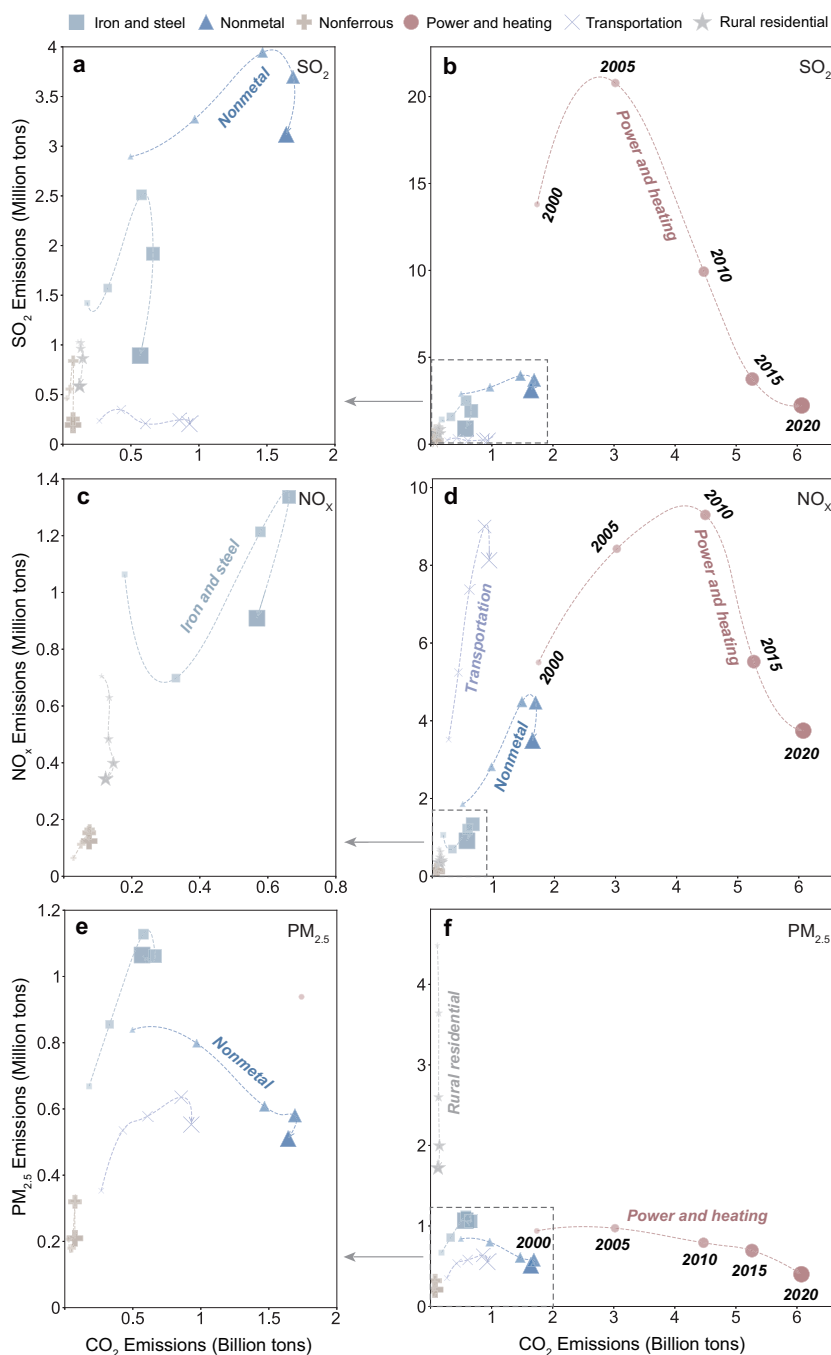
**Fig. 1 | Trends in air pollutant and CO<sub>2</sub> emissions across China during 2000–2020.** **a** Estimated national anthropogenic emissions of SO<sub>2</sub>, NO<sub>x</sub>, primary PM<sub>2.5</sub>, and CO<sub>2</sub> by 15 socioeconomic sectors. **b** Variations in national GDP and emissions of air pollutants and CO<sub>2</sub>, relative to the year 2000. **c** Overview of key energy, climate, and environmental control policies implemented from 2000 to 2020 in China. Note: in (c), Phase I Action Plan represents the Air Pollution Prevention and Control Action Plan; Phase II Action Plan represents the Three-Year Action Plan for Winning the Blue Sky Defense Battle; Double Carbon target represents the carbon peaking and carbon neutrality targets; De-S refers to desulfurization; De-N refers to denitrification; and NG refers to natural gas.



two decades, notable progress was made in curbing air pollutant emissions across China, while sectoral CO<sub>2</sub> emissions showed a general upward or modest decreasing trend. As a result, the relationship in sectoral pollutant-CO<sub>2</sub> emissions exhibited temporally divergent characteristics, which are closely related to the distinct timeline of implementing pollutant-specific environmental control and energy and climate policies.

During the early stage (2000–2005), co-growth trends in pollutant-CO<sub>2</sub> emissions were observed in most key sectors as driven by surging energy and production demands and limited pollution control and decarbonization efforts (Fig. 1c). With the ongoing reinforcement of end-of-pipe controls, sectoral pollutant-CO<sub>2</sub> emission relationships began to exhibit noticeable diverging trends from 2005 to 2010. Specifically, a trade-off between SO<sub>2</sub> and

**Fig. 2 | Synergetic trends in emissions of major air pollutants and CO<sub>2</sub> across key sectors in China from 2000 to 2020. a, b SO<sub>2</sub>, c, d NO<sub>x</sub>, and e, f PM<sub>2.5</sub>.** Note: dots are colored by different sectors, and their sizes (or color intensity) correspond to the year, ranging from the smallest (or lightest) for 2000 and the largest (or darkest) for 2020.



CO<sub>2</sub> emissions in the power and heating sector was observed. This phenomenon can be largely attributed to the installation of flue-gas desulfurization (FGD) equipment in coal-fired power plants mandated by the Chinese government in 2006 (Fig. 1c)<sup>33,36</sup>, which effectively improved the removal efficiency of SO<sub>2</sub> emissions in coal-fired power plants (i.e., from 8% in 2005 to 78% in 2010)<sup>35</sup>, leading to a substantial 52.2% reduction in sectoral SO<sub>2</sub> emissions. However, co-growth trends in air pollutant and CO<sub>2</sub> emissions were witnessed in several energy-intensive sectors, such as the co-growth of NO<sub>x</sub> and CO<sub>2</sub> emissions in the power and heating sector, and the co-growth of all three major air pollutant and CO<sub>2</sub> emissions in the transportation sector and the iron and steel sector. Such co-growth trends could mainly be attributed to the rapid increase in activity levels.

Between 2010 and 2015, trade-offs favoring air pollution control were observed in more sectors and covered more species, reflecting the stricter pollution control policies. For example, disparate patterns between NO<sub>x</sub> and

CO<sub>2</sub> emissions were witnessed in the power and heating sector, in which sectoral CO<sub>2</sub> emissions grew by 17.8%, while NO<sub>x</sub> emissions declined by 40.6%, under the background that the national electricity generation from thermal power plants increased by 28.6% during 2010–2015<sup>37</sup>. This divergence oriented by clean air priorities could be explained by the joint effect of the widespread adoption of denitrification technologies and phasing-out of small and outdated power generation units, as illustrated in Fig. 1c<sup>34,38</sup>. Additionally, stricter post-2010 environmental control policies prompted the installation of FGD equipment in the industrial sector (Fig. 1c)<sup>39</sup>, leading to, for example, a 23.6% decline in SO<sub>2</sub> emissions from the iron and steel sector during 2010–2015, thus revealing a contrasting SO<sub>2</sub> and CO<sub>2</sub> emission trend in the iron and steel sector. However, the transportation sector still experienced a continuous co-growth trend in NO<sub>x</sub>-CO<sub>2</sub> emissions during this phase, driven by the ongoing increase in the vehicle population (i.e., increase by 45.3% during 2010–2015)<sup>37</sup>.

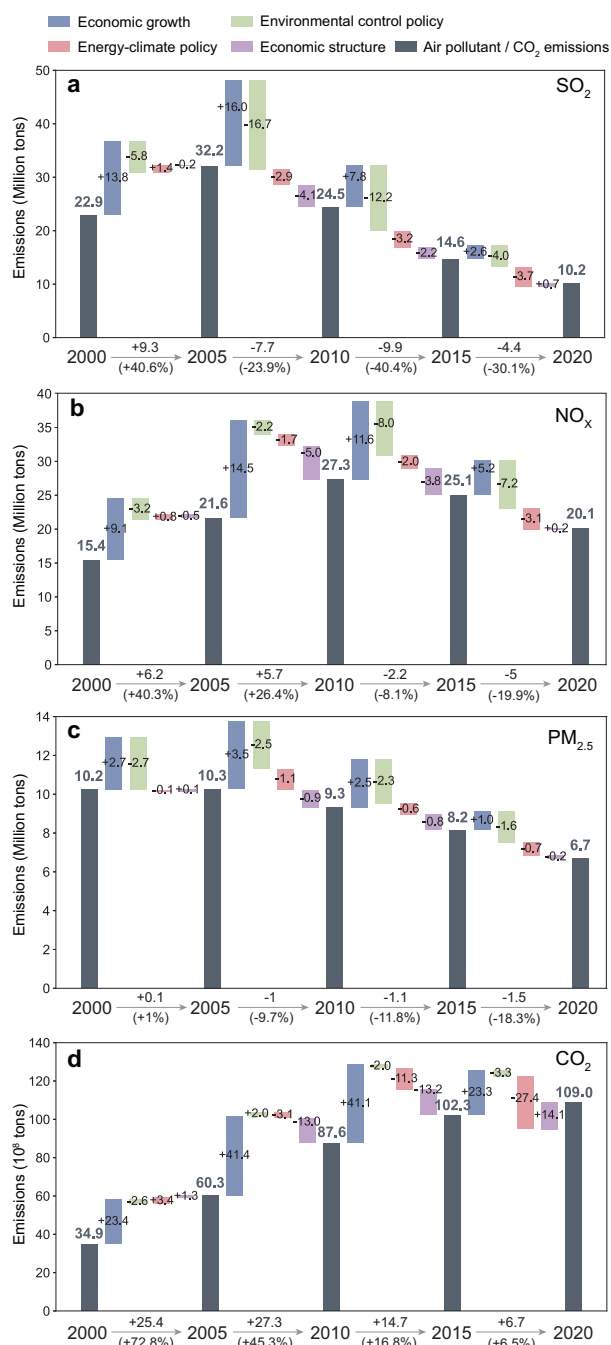


**Fig. 3 | Drivers for changes in emissions of major air pollutants and CO<sub>2</sub> across China during 2000–2020.** Panels represent the impacts of drivers on national air pollutant and CO<sub>2</sub> emissions: **a** SO<sub>2</sub>, **b** NO<sub>x</sub>, **c** PM<sub>2.5</sub>, and **d** CO<sub>2</sub>.

During the latest investigated period (2015–2020), the positive synergy evolution pattern emerged in several key industrial sectors (e.g., the iron and steel sector, the nonmetal sector represented by cement production, and the nonferrous metal sector led by aluminum production), as well as the rural residential sector. This positive pattern can be attributed to the efficacy of implementing structural adjustment measures during the Phase II Action Plan period (i.e., 2018–2020)<sup>40</sup>. For example, the rural residential sector experienced an evident co-mitigation of primary PM<sub>2.5</sub> and CO<sub>2</sub> emissions from 2015 to 2020, largely driven by a 34% reduction in coal consumption (Supplementary Fig. S3), suggesting that the clean heating program implemented in northern China since 2017 has greatly accelerated the transition toward cleaner energy sources (e.g., natural gas and electricity) in

rural households (Fig. 1c)<sup>41</sup>. In addition, another crucial factor to facilitate synergistic reductions may include the contraction of industrial and socio-economic activities, predominantly driven by the COVID-19 lockdown in 2020<sup>42</sup>. However, during this period, opposing trajectories in pollutant-CO<sub>2</sub> emissions persisted in the power and heating sector, as well as in the NO<sub>x</sub>-CO<sub>2</sub> relationship in the transportation sector, driven by increased demand and increasingly strengthened pollutant control measures. For example, NO<sub>x</sub> emissions in the transportation sector were estimated to decrease by 9.7% from 2015 to 2020, which can be primarily attributed to the upgrading of vehicle emission standards (e.g., the implementation of China V in 2017) and changes in travel behavior (e.g., modal shift from road to rail and waterways)<sup>28,43</sup>, as shown in Fig. 1c, while CO<sub>2</sub> emissions continued to rise (that is, 8.7% increase). These divergent patterns indicate that the upward trajectory of sectoral CO<sub>2</sub> emissions has yet effectively curbed by current decarbonization efforts. Therefore, co-reduction strategies targeting pollutant-CO<sub>2</sub> emissions from key sectors (e.g., large emission contributors) require a challenging shift toward reinforced low-carbon actions. Such strategies would adopt a more comprehensive structural approach than conventional pollution control measures.

### Co-drivers of air pollutant and CO<sub>2</sub> emissions

Figure 3 shows the synergistic effects of four aggregated socioeconomic drivers on changes in air pollutant and CO<sub>2</sub> emissions across China. Economic growth (blue bars in Fig. 3) was identified as the key co-driver behind evident co-growth in air pollutant and CO<sub>2</sub> emissions across the whole period. However, since the 11<sup>th</sup> FYP period, as China embraced a new normal development phase characterized by a slowing pace of economic growth, the effect of economic growth on driving the co-growth of air pollutant and CO<sub>2</sub> emissions has progressively weakened. Between 2015 and 2020, increases in total emissions of SO<sub>2</sub>, NO<sub>x</sub>, primary PM<sub>2.5</sub>, and CO<sub>2</sub> driven by economic growth have reduced by 86–92.5% compared to the period of 2000–2015.

Environmental control policies (green bars in Fig. 3), which focused on lowering emission intensity primarily through the deployment of end-of-pipe control and applying advanced production technologies, largely offset the increasing emissions of all three air pollutants driven by economic growth. Overall, this factor successfully reduced SO<sub>2</sub>, NO<sub>x</sub>, primary PM<sub>2.5</sub>, and CO<sub>2</sub> emissions by 169.3%, 133.3%, 88.6%, and 16.8% during 2000–2020, respectively. However, trends of its effects varied greatly across species, reflecting the evolving control priorities. Specifically, from 2005 to 2010, environmental control policies demonstrated effective in curbing the increasing trends in SO<sub>2</sub> emissions of 51.9%, due to ~86% of the coal-fired power plants, which are the largest SO<sub>2</sub> emission contributor, carried out FGD retrofits during the 11<sup>th</sup> FYP period (Fig. 1c)<sup>33</sup>. As a result, the potential to further reduce SO<sub>2</sub> emissions through environmental control policies progressively reduced in the subsequent stages. In contrast, the impact of environmental control policies in reducing NO<sub>x</sub> emissions emerged after 2010, owing to the implementation of the total NO<sub>x</sub> emissions control policy (i.e., a 10% reduction in NO<sub>x</sub> emissions from 2010 to 2015). Consequently, a series of measures have been implemented primarily focusing on end-of-pipe NO<sub>x</sub> emission control<sup>34</sup>. For example, over 80% of power plants were equipped with advanced denitrification devices by 2015, and over 80% of sintering facilities and clinker kilns were equipped with similar technologies by the end of 2017<sup>24</sup>. As the emission reduction potential from end-of-pipe control shrinks, pollutant emission reductions driven by environmental control policies diminished a lot in the latest period of 2015–2020 (Fig. 3).

As the efficacy of environmental control policies gradually weakened, energy-climate policies (pink bars in Fig. 3) aimed at optimizing the energy structure and reducing energy intensity, increasingly played a crucial role in co-mitigating air pollutant and CO<sub>2</sub> emissions. Specifically, the energy-climate policies first contributed to mitigating the co-growth in air pollutant and CO<sub>2</sub> emissions from 2005 to 2010, driven by the energy intensity reduction targets of 20% mandated in the 11<sup>th</sup> FYP period<sup>33</sup>. This effect successfully co-reduced emissions of SO<sub>2</sub>, NO<sub>x</sub>, primary PM<sub>2.5</sub>, and CO<sub>2</sub> by 9%, 7.6%, 10.4%, and 5.1%, respectively, compared to the 2005 level. This

positive synergy was primarily achieved due to the widespread adoption of energy-saving technologies (e.g., low-temperature waste heat recovery technology in the cement industry)<sup>44</sup>. In the following decade, energy-climate policies further intensified synergetic downward trends in SO<sub>2</sub>, NO<sub>x</sub>, primary PM<sub>2.5</sub>, and CO<sub>2</sub> emissions of 28.1%, 18.8%, 13.5%, and 44.1% from 2010 to 2015, respectively, and successfully offset the economic-growth-driven increases in SO<sub>2</sub> and CO<sub>2</sub> emissions during 2015–2020. The progressively intensified efficacy of energy-climate policies was propelled by 16% and 15% energy intensity reduction targets during the 12<sup>th</sup> and 13<sup>th</sup> FYP periods, respectively, as well as persistent efforts in promoting the energy structure transition<sup>34,38,40,45</sup>. For example, the share of coal consumption decreased by 20.7% from 2010 to 2020, while the proportion of gaseous fuels nearly doubled (Fig. S4).

The economic structure effect (purple bars in Fig. 3) characterized by the industrial transition and upgrading, generally contributed to co-reductions of air pollutants and CO<sub>2</sub>, despite the effects showing a

fluctuating trend over time. This fluctuation is primarily driven by the relative contribution of energy-intensive industries to the overall economy across different phases. From 2005 to 2015, the GDP share of heavy industries declined by 6.3%, while the proportion of the tertiary sector increased by 26.2%, leading to co-reductions in SO<sub>2</sub>, NO<sub>x</sub>, primary PM<sub>2.5</sub>, and CO<sub>2</sub> emissions of 19.4%, 40.7%, 16.5%, and 43.5%, respectively. Notably, this driver exhibited positive effects on emission growth from 2015 to 2020. This phenomenon can be explained by the change in key emission sources, with the nonmetal and transportation sectors gradually replacing the industrial sector as major contributors to national SO<sub>2</sub> and NO<sub>x</sub> emissions, respectively (Fig. 1a). Additionally, due to the economic recession impacted by the COVID-19 pandemic, energy-intensive industries were prioritized to combat the economic slump, thereby exacerbated emissions during this period<sup>42</sup>. For example, a notable increase in total industrial GDP shares of the power and heating sector (40%) and the nonmetal sector (23.2%) was reported (Supplementary Fig. S5)<sup>46</sup>.

**Table 1 | Clusters of provinces based on air pollution and CO<sub>2</sub> co-control characteristics**

Clusters	Province counts	Provinces
Cluster 1	4	Beijing, Tianjin, Jiangsu, and Zhejiang
Cluster 2	3	Guangdong, Shanghai, and Fujian
Cluster 3	3	Xinjiang, Ningxia, and Hainan
Cluster 4	3	Heilongjiang, Jilin, and Liaoning
Cluster 5	3	Sichuan, Qinghai, and Yunnan
Cluster 6	8	Hebei, Henan, Shandong, Shanxi, Shaanxi, Gansu, Chongqing, and Hunan
Cluster 7	6	Anhui, Hubei, Inner Mongolia, Jiangxi, Guangxi, and Guizhou

**Regional heterogeneity in co-drivers of air pollutant and CO<sub>2</sub> emissions**

The regional disparities in economic development levels across China, coupled with the varying industrial structure and the uneven progress in implementing emission control strategies, lead to differentiated regional pollution-carbon co-control characteristics. Based on the Gaussian Mixture Model (GMM) clustering method, China’s 30 provinces are grouped into seven clusters, as shown in Table 1 and the spatial distribution map in Fig. 4, with the radar charts further illustrating the influence of drivers on air pollutants and CO<sub>2</sub> emission changes, as well as the co-driving effects. Generally, the impacts of co-drivers demonstrate notable regional heterogeneity. From 2000 to 2020, regions that achieved relatively substantial emission reductions are mainly located in the Beijing-Tianjin-Hebei (BTH) and surrounding regions, Yangtze River Delta (YRD), and central China (i.e., regions in Clusters 1, 2, and 6 of Fig. 4).

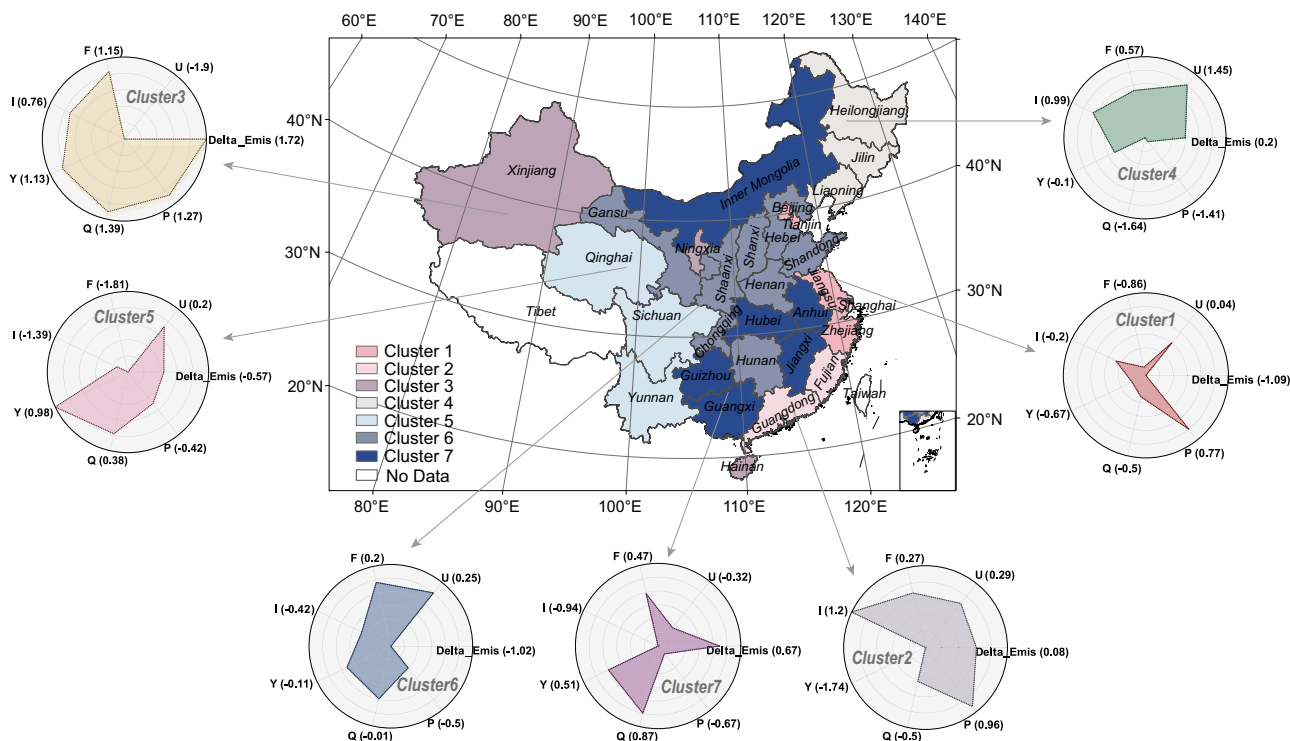


**Fig. 4 | Heterogeneity in co-control characteristics of major air pollutants and CO<sub>2</sub> across provincial clusters during 2000–2020.** Map: spatial distribution of provinces in different clusters, based on the Gaussian Mixture Model (GMM) clustering method. Radar graphs: the impacts of drivers on air pollutant and CO<sub>2</sub> emission changes across different types of provinces during 2000–2020. Note: U, F,

I, Y, Q, P, and Delta\_Emis represent emission intensity, energy structure, energy intensity, economic structure, per capita GDP, population, and changes in air pollutant and CO<sub>2</sub> emissions, respectively. The results in parentheses represent the relative contributions of drivers to emission changes and the absolute changes in air pollutant and CO<sub>2</sub> emissions, which are based on Z-score standardized processing.

Cluster 1 includes Beijing, Tianjin, Jiangsu, and Zhejiang, which are all economically advanced provinces in China. In this cluster, energy structure, energy intensity, and economic structure were witnessed to generate positive effects on driving air pollutant and CO<sub>2</sub> emission co-reductions. For example, strengthened energy efficiency policies synergistically reduced NO<sub>x</sub>, primary PM<sub>2.5</sub>, and CO<sub>2</sub> emissions by 32.7%, 21.4%, and 83.1% during 2000–2020, respectively. This effectiveness can be attributed to the adoption of advanced and cleaner industrial production technologies through financial subsidies and economic incentives<sup>47</sup>. For instance, Beijing's strategic integration of green building practices and energy-efficient appliances exemplifies successful energy-saving technology diffusion supported by targeted subsidies<sup>48</sup>. However, this localized action that effectively reduces energy intensity has not been implemented nationwide.

Cluster 2 consists of coastal regions with relatively advanced economic development, characterized by rapid urbanization and a concentration of high-tech industries. The transformation in economic structure exerted a critical suppressive effect on the augmentation of air pollutant and CO<sub>2</sub> emissions, as illustrated in Fig. 4. Specifically, industrial structure transformation and upgrading policies adopted in Cluster 2 drove substantial co-reductions of 82.3% in SO<sub>2</sub>, 117.1% in NO<sub>x</sub>, 42.9% in primary PM<sub>2.5</sub>, and 155.1% in CO<sub>2</sub> emissions during 2000–2020, respectively (Supplementary Fig. S6). This success can be explained by actions fostering the growth of innovative high-tech industries (e.g., Information and Communication Technology industry) and service sectors. A representative case is Shanghai in the YRD region, where the share of the secondary industry declined by 42.8%, while the proportion of the tertiary industry increased by 40.1% during this period<sup>49</sup>.

Cluster 3 comprises Xinjiang, Ningxia, and Hainan. Xinjiang and Ningxia, key bases for coal chemical industries and oil extraction in China, remain heavily dependent on traditional fossil fuels to sustain their energy supply. As a result, the co-reduction of air pollutant and CO<sub>2</sub> emissions has been hindered by the overall negative effects of the energy structure. For instance, the energy structure effect contributed to a modest 1.6% decrease in SO<sub>2</sub> emissions while increasing CO<sub>2</sub> emissions by 5.1%. Additionally, the positive impact of energy intensity on emission increases in Cluster 3 is mainly the consequence of the industrial energy utilization efficiency lagging behind the pace of industrialization.

Provinces in Cluster 4 (i.e., Heilongjiang, Jilin, and Liaoning located in northeastern China) are recognized as traditional heavy industrial hubs. This cluster encounters unique challenges in attaining pollution-carbon co-control due to its entrenched industrial structure dominated by resource-intensive sectors and delayed technological upgrades. In contrast to other provincial clusters, energy structure and energy intensity have demonstrated relatively negative impacts on achieving synergetic reductions in Cluster 4. For example, the energy intensity effect led to notable upward trends in SO<sub>2</sub> and NO<sub>x</sub> emissions in Cluster 4 during 2000–2020 (40.7% and 39.2%, respectively), as shown in Supplementary Fig. S6. This indicates that regions in Cluster 4 remain critical bottlenecks in advancing energy efficiency. Additionally, the effectiveness of end-of-pipe control measures in reducing PM<sub>2.5</sub> emissions (that is, averaged at a 61.4% removal rate) exhibited relatively limited compared to other provincial groups, largely due to the relatively lenient emission standards for PM in this cluster<sup>50</sup>.

For regions in Cluster 5 (that is, Sichuan, Qinghai, and Yunnan), the optimization of the energy structure was proven to be more effective in driving co-reductions compared to other provincial groups (Fig. 4). From 2000 to 2020, this driver effectively co-reduced SO<sub>2</sub>, NO<sub>x</sub>, primary PM<sub>2.5</sub>, and CO<sub>2</sub> emissions of 29.4%, 23.5%, 5.2%, and 60.3%, respectively. Provinces in this group have progressively integrated renewable energy sources as a key component of their energy supply systems, owing to the local endowment with abundant renewable resources (e.g., wind power, hydro-power, and photovoltaic energy). Specifically, the share of renewable energy (excluding biomass) in the energy mix of Cluster 5 increased from 1.7% in 2000 to 10.7% in 2020 (Supplementary Fig. S7).

Cluster 6 covers eight provinces, with five concentrated in central China (Fig. 4). As a result of the synergetic effects of industrial restructuring

and energy efficiency improvement, this cluster has made progress in co-reducing air pollutant and CO<sub>2</sub> emissions. Specifically, cumulative synergetic reductions of 56.8%, 94.6%, 36.1%, and 135.6% were observed for SO<sub>2</sub>, NO<sub>x</sub>, primary PM<sub>2.5</sub>, and CO<sub>2</sub> emissions during 2000–2020, respectively, driven by the combined effects of energy intensity and economic structure. In general, Cluster 6 presents three distinct industrial profiles. Shanxi, Shaanxi, and Gansu are resource-intensive regions with coal-dominated production systems, while Shandong, Hebei, Henan, and Hunan serve as critical manufacturing centres known for energy-intensive industries (e.g., iron and steel, cement, and glass production). Chongqing is distinguished by its relatively developed automobile and machinery manufacturing industries. Despite these industrial divergences, a common challenge across these provinces lies in their coal-dominated energy consumption patterns. For example, it was estimated that the energy structure effect contributed only 8.1%, 9.8%, and 17% to reductions in SO<sub>2</sub>, NO<sub>x</sub>, and CO<sub>2</sub> emissions, respectively, much lower than the national average results (10–25.4%). This suggests that optimizing the energy mix in this cluster holds substantial potential in driving future emission reductions.

Cluster 7 demonstrates an “efficiency-driven” characteristic of pollution-carbon co-control. As shown in Fig. 4, improvements in both energy and emission efficiency were witnessed to effectively curb the growth of air pollutant and CO<sub>2</sub> emissions. Specifically, the combined impacts of emission intensity and energy intensity substantially co-mitigated SO<sub>2</sub>, NO<sub>x</sub>, primary PM<sub>2.5</sub>, and CO<sub>2</sub> emissions of 220.3%, 202%, 108.6%, and 166% during 2000–2020, respectively. In contrast, an evident trade-off driven by the effects of energy and economic structures was observed, with the economic structure effect even exacerbating the increase in SO<sub>2</sub> (0.7%) and CO<sub>2</sub> (31.4%) emissions (Supplementary Fig. S6). This phenomenon can be explained by the slow pace of traditional industrial upgrading, coupled with the relocation of industries from the eastern coastal regions to the central and western parts of China, a shift that was promoted by official guidelines issued in 2010<sup>51</sup>.

## Discussion

In this study, we evaluate the synergetic evolution patterns of air pollutant and CO<sub>2</sub> emissions across China based on an emission inventory categorized by detailed sectoral sources. Socioeconomic and policy co-drivers behind these patterns were further identified based on the LMDI index decomposition analysis. Subsequently, we analyze the spatial heterogeneity in co-control characteristics of air pollutant and CO<sub>2</sub> emissions, using the clustering technique. Our analysis indicates that despite historical policies have successfully curbed air pollutant emissions over China, CO<sub>2</sub> emission control remains a notable challenge. Efforts to optimize the energy structure and reduce energy intensity are increasingly pivotal in driving the co-mitigation of air pollutant and CO<sub>2</sub> emissions. For example, the transition towards a cleaner energy system holds substantial potential for attaining co-control in renewable-resource-rich regions, whereas improvements in energy efficiency have been demonstrated to be particularly effective in areas dominated by energy-intensive industries. Based on the synergetic evolution of sectoral pollutant-CO<sub>2</sub> emissions and disparities in pollution-carbon co-control characteristics across different provincial groups, we provide several implications for formulating future region-specific co-control strategies. Details of uncertainties and limitations can be found in Supplementary Text S3.

Future regional co-control actions could be guided by the successful practices of regions that have achieved substantial co-reductions driven by historical policy interventions. Characterized by developed economies and dense populations, regions in Clusters 1 and 2 have made notable strides in co-reducing air pollutant and CO<sub>2</sub> emissions, driven by relatively low-carbon industrial profiles (Fig. 4). Empirical studies have similarly highlighted the pivotal role of industrial restructuring in advancing synergetic efficiency, particularly in developed coastal regions<sup>16,26</sup>. This suggests that effective structural strategies including fostering emerging service and high-value-added sectors (e.g., electronic information, biopharmaceuticals), eliminating inefficient capacity in traditional energy-intensive industries (e.g., the iron

and steel, cement), and promoting green building practices in the construction sector through supply-side reforms, could be maintained and progressively reinforced in these economically advanced regions to sustain co-reduction benefits<sup>52,53</sup>. Our analysis also reveals that in regions dominated by energy-intensive industries, where rapid industrial substitution remains challenging, strategies driven by energy efficiency improvements serve as a feasible alternative route for co-control, as evidenced by the successful experiences witnessed in regions in Clusters 5, 6, and 7 (Fig. 4). We recommend that future strategies could prioritize the application of clean energy production and high-efficiency industrial technologies in energy-intensive regions, with targeted economic incentives acting as a catalyst for technological innovation. The effectiveness of technological innovation in driving co-reductions has also been documented in prior studies<sup>54,55</sup>. For instance, the promotion of precalciner kilns in cement production and the deployment of advanced waste heat recovery technology in the iron and steel sector have been proven to synergetically mitigate emissions<sup>39,56,57</sup>. As China's recent efforts to scale up policy-driven financial mechanisms to support industrial technological upgrading, strategies targeting manufacturing technologies breakthroughs (e.g., innovation in electric vehicle systems) manifest considerable prospects for synergetic control<sup>58,59</sup>.

Additionally, coal-based fossil fuel consumption is acknowledged as the primary source of air pollutant and CO<sub>2</sub> emissions. However, curbing emissions from coal-based energy systems remains essential, while effective policy responses could also focus on propelling the renewable energy transition, particularly in fossil fuel-dependent regions with relatively weak economic foundations. Our analysis underscores the potential of expediting the green transformation of energy systems as a promising strategy to attain co-control in resource-intensive regions (Cluster 5 in Fig. 4), aligning with previous research findings<sup>60</sup>. China has pledged to increase the share of non-fossil energy consumption to exceed 80% by 2060 and issued a series of policy directives intended to promote the development of photovoltaic and wind energy technologies across western regions<sup>61,62</sup>. Thereby, in regions endowed with abundant renewable resources, it is worthwhile to investigate strategies that facilitate the clean transition of coal-based energy supply and industrial systems during the ongoing industrialization process, such as constructing large-scale wind and photovoltaic power bases<sup>63</sup>. Moreover, the interregional transmission of surplus clean energy could serve as a complementary approach toward optimizing resource allocation and maximizing the utilization efficiency of renewable resources, as demonstrated by the success of the West to East Power Transmission Project<sup>64</sup>.

In contrast, regions facing challenges in delivering satisfactory co-reduction outcomes could benefit from overcoming internal deficiencies while drawing on successful mitigation experiences demonstrated elsewhere. Specifically, in economically lagging regions where energy-intensive manufacturing or legacy heavy industries remain dominant (regions in Clusters 3, 4, and 7), special attention could be paid to avoiding a development pathway featured by early pollution surges, followed by delayed or insufficient mitigation efforts. We suggest that near-term co-control efforts in these regions could prioritize deploying high-efficiency end-of-pipe control technologies and mandating more rigorous emission standards across less targeted regions. For example, the early enforcement of “ultra-low” emission standards in the power sector has been demonstrated to yield remarkable air quality and health benefits in the YRD region<sup>65</sup>. Given the diminishing effectiveness of end-of-pipe controls as a mitigation strategy, a shift towards a sustainable and low-carbon development trajectory of industrial and energy structures could be actively pursued to attain long-term co-mitigation<sup>66,67</sup>. Future initiatives might focus on the context-sensitive transfer of sector-specific structural reform strategies that have demonstrated effective in other regions, such as facilitating the transition from traditional blast furnace-basic oxygen furnace (BF-BOF) to electric arc furnace (EAF) in the iron and steel sector, resolving excess production capacity in the cement industry, and developing a new power system driven by renewable energy in the power and heating sector. These measures have been demonstrated to synergetically deliver notable benefits in improving air quality and associated public health, as well as mitigating climate change<sup>68–70</sup>.

Notably, despite these efforts, achieving co-control remains challenging due to uneven progress in the pace of transition efforts across different provincial groups. For example, regions where economies are heavily reliant on resource extraction have long featured an energy portfolio dominated by coal. As coal serves as the foundation of regional economic development, efforts toward energy system transitions continue to encounter formidable resistance<sup>71</sup>. Additionally, the high financial burden associated with technological innovations and equipment upgrades would hinder industrial upgrading efforts in regions that are characterized by heavy reliance on energy-intensive industries and legacy infrastructure<sup>47</sup>. Therefore, locally adapted incentives and inter-regional industrial transfer policies are required to further unlock the potential for co-control.

Overall, this analysis comprehensively identifies spatial and sectoral disparities in the co-evolution of air pollutant and CO<sub>2</sub> emissions across China and guides the formulation of more effective policies to attain synergies in mitigating emissions. The summarized experiences from co-mitigation strategies across different provincial types are also applicable internationally, particularly for developing countries undergoing similar developmental stages and environmental challenges.

## Methods

### Research framework

Supplementary Fig. S8 shows the schematic of our integrated research framework. The framework is structured into four main parts. First, the GAINS-China model is used as an anthropogenic air pollutant and CO<sub>2</sub> emission inventory and serves as the basis for subsequent decomposition and clustering analyses. Key parameters in the GAINS-China model are calibrated, including socioeconomic data, energy consumption, and material production, as well as pollutant-specific implementation rates of end-of-pipe control technologies, ensuring that the activity level data genuinely reflects the actual conditions in China. Correspondingly, the anthropogenic emission inventory of three major air pollutants (i.e., SO<sub>2</sub>, NO<sub>x</sub>, and PM<sub>2.5</sub>) and CO<sub>2</sub> across China is updated for the period 2000–2020, at five-year intervals. Based on historical emission trends, we analyze the synergetic patterns of air pollutant and CO<sub>2</sub> emissions across temporal and sectoral dimensions. Second, the Logarithmic Mean Divisia Index (LMDI) decomposition method is applied to identify the socioeconomic and policy drivers contributing to the temporal changes in historical air pollutant and CO<sub>2</sub> emission patterns. Third, the relative contributions of six driving factors to emission changes and absolute changes in air pollutant and CO<sub>2</sub> emissions are used together as clustering variables for the 30 provincial samples. Finally, based on the decomposed drivers, principal component analysis (PCA) coupled with the Gaussian Mixture Model (GMM) clustering method is applied to categorize China's provinces into different groups. Based on the clustering results, we identify pollution-carbon co-control characteristics across different provincial groups and propose tailored co-control strategies at the regional level.

### Data collection and update of the GAINS-China dataset

Elaborating data on provincial and sectoral energy consumption, air pollutant, and CO<sub>2</sub> emissions, as well as socioeconomic statistics, serves as crucial input to support the decomposition of driving forces behind anthropogenic emission trends. Provincial air pollutant and CO<sub>2</sub> emissions from detailed source categories, as well as the corresponding sector-specific activity rates (e.g., energy consumption or material production) for the period 2000–2020, with an interval of 5 years, are obtained from the GAINS-China model<sup>72,73</sup>. To improve the model's reliability in performing China's actual situations, we update and calibrate the provincial activity level data for the year 2020 in the GAINS-China model, including energy consumption (e.g., consumption of coal, liquid fuels, gaseous fuels, and natural gas) and material production (e.g., crude steel, pig iron, cement, and glass) from detailed source categories. The updates are based on statistics retrieved from the China Energy Statistics Yearbook, provincial statistical yearbooks, ecological and environmental statistics from the MEE, as well as the Carbon Emission Accounts and Datasets (CEADs)<sup>74,75</sup>. Additionally, the pollutant-specific implementation rates of end-of-pipe control technologies are

calibrated using data obtained from ecological and environmental statistics. Details on updating the GAINS-China dataset are available in Supplementary Text S1. Finally, we establish a mapping process between the detailed source categories defined in the GAINS model and socioeconomic sectors, allowing us to classify anthropogenic emissions of major air pollutants and CO<sub>2</sub> into 15 final socioeconomic sectors. These sectors include 13 commercial subsectors, as well as the urban and rural residential sectors (Supplementary Table S1).

Socioeconomic statistics for years 2000, 2005, 2010, and 2020, such as provincial GDP, province-, and sector-specific GDP, as well as population data, are derived or estimated based on official statistical yearbooks compiled by the National Bureau of Statistics of China (NBS). The estimated GDP values of industrial subsectors are constrained by the total industrial GDP at the provincial level and the share of subsector GDP in the national industrial GDP. The sectoral price index, retrieved from the China Price Index Statistical Yearbook, is further applied to deflate the GDP dataset at 2000 constant prices<sup>76</sup>. Details on the processing of provincial and sectoral GDP can be found in Supplementary Text S2.2.

### Synergy or trade-off between air pollutant and CO<sub>2</sub> emissions

Synergy is theoretically characterized by the simultaneous evolution of two separate systems toward a superior state<sup>77–79</sup>. In our study, we extend this concept to qualitatively evaluate the relationship between air pollutant and CO<sub>2</sub> emissions using a two-dimensional synergetic coordinate system, as shown in Supplementary Fig. S9. Specifically, positive synergy (Quadrant III in Supplementary Fig. S9) refers to the co-reduction of air pollutant and CO<sub>2</sub> emissions driven by environmental control or climate policy interventions, implying a “win-win” outcome that simultaneously benefit air quality improvement and climate mitigation<sup>80</sup>. Conversely, negative synergy (Quadrant I in Supplementary Fig. S9) occurs when such interventions lead to the co-growth in pollutant-carbon emissions, demonstrating a “mutual detriment” outcome of air quality and climate<sup>81</sup>. Beyond positive and negative synergies, two types of trade-off evolution are identified when policy measures benefit one or the other. A trade-off favoring clean air (Quadrant II in Supplementary Fig. S9) is observed when air pollutant emissions decline while CO<sub>2</sub> emissions increase, whereas a trade-off favoring low-carbon (Quadrant IV in Supplementary Fig. S9) reflects CO<sub>2</sub> reductions accompanied by rising air pollutant emissions. Additionally, we evaluate synergetic effects by decomposing the contributions of socioeconomic and policy factors to air pollutant and CO<sub>2</sub> emission changes in a certain period. Synergy occurs when the effects on air pollutants and CO<sub>2</sub> emissions are directionally aligned and even comparable in magnitude. Otherwise, the pollutant-CO<sub>2</sub> relationships are manifested as trade-offs.

### The LMDI decomposition method

The LMDI approach is used to decompose the contributions of driving factors to emission changes in each air pollutant and CO<sub>2</sub> across China’s 30 provinces during 2000–2020, with a 5-year interval. As one of the most widely used methods for index decomposition analysis (IDA), the LMDI approach has gained popularity in investigating the driving mechanisms behind energy consumption, air pollutant and CO<sub>2</sub> emissions, PM<sub>2.5</sub> exposure, and related health burdens due to its consistency in aggregation<sup>25,82–84</sup>. Its independent decomposition structure effectively avoids unexplained residual terms and ensures that the results remain dimensionless in the decomposition process<sup>85–87</sup>. Details regarding the LMDI decomposition method are provided in Supplementary Text S2.3.

Given the distinct emission patterns from different sectoral sources, emissions of three major air pollutants and CO<sub>2</sub> from the 15 final socioeconomic sectors are classified into three categories, which can be expressed as follows:

$$Emis_{total} = Emis_{ene} + Emis_{non-ene} + Emis_{res} \quad (1)$$

where  $Emis_{ene}$  represents emissions from 13 commercial subsectors related to fuel combustion,  $Emis_{non-ene}$  represents emissions from non-energy

processes in 13 commercial subsectors, and  $Emis_{res}$  denotes emissions from urban and rural residential sectors.

Then, emissions from three source categories are decomposed into multiple specific driving factors as follows:

$$\begin{aligned} Emis_{ene} &= \sum_s \sum_f (C_{s,f}/E_{s,f}) * (E_{s,f}/E_s) * (E_s/A_s) * (A_s/A) * (A/P) * P \\ &= \sum_s \sum_f U_{s,f} F_{s,f} I_s Y_s QP \end{aligned} \quad (2)$$

$$Emis_{non-ene} = \sum_s (C_s/A_s) * (A_s/A) * (A/P) * P = \sum_s U_s Y_s QP \quad (3)$$

$$\begin{aligned} Emis_{res} &= \sum_s \sum_f (C_{s,f}/E_{s,f}) * (E_{s,f}/E_s) * (E_s/P_s) * P_s \\ &= \sum_s \sum_f U_{s,f} F_{s,f} I_s P_s \end{aligned} \quad (4)$$

where  $s$  and  $f$  represent different sectors and fuel types, respectively, and the fuel type includes coal, liquid fuels, gaseous fuels, and natural gas;  $C$ ,  $E$ ,  $A$ , and  $P$  refer to emissions, energy consumption, economic development level (i.e., GDP), and population, respectively.  $P_s$  represents the population number in the urban or rural residential sector. According to Eqs. (2)–(4),  $U$  denotes the emission intensity, which is characterized as emissions generated per unit of fuel consumed in Eqs. (2) and (4) and emissions per unit of GDP in Eq. (3), which is primarily influenced by environmental control measures.  $F$  denotes the energy consumption structure, which is defined as the fractional contribution of each energy type to the total energy consumption.  $I$  represents the energy intensity, which demonstrates the energy consumption per unit of GDP in Eq. (2) and per capita energy consumption in Eq. (4).  $Y$  represents the changes in economic structure, indicating the contribution of each sector to regional GDP.  $Q$  represents the economic growth level, which is defined as GDP per capita.

Based on the LMDI additive decomposition method, the aggregated effects of each driver on emission changes are calculated by summing the fuel- and sector-specific decomposition results across three source categories (i.e.,  $Emis_{ene}$ ,  $Emis_{non-ene}$ , and  $Emis_{res}$ ). Provincial emission changes between the year 2000 and the target year  $T$  can be decomposed as Eq. (5). The national decomposition results are obtained by aggregating the provincial-level results.

$$\begin{aligned} \Delta Emis_{s,f}^{T-2000} &= Emis_{s,f}^T - Emis_{s,f}^{2000} \\ &= \sum_s \sum_f (\Delta U_{s,f}^{T-2000} + \Delta F_{s,f}^{T-2000} + \Delta I_s^{T-2000} + \Delta Y_s^{T-2000} + \Delta Q^{T-2000} + \Delta P^{T-2000}) \end{aligned} \quad (5)$$

Emission variations contributed by each driving factor on the right side of Eq. (5) can be further decomposed according to the LMDI method. Taking the emission efficiency  $U$  ( $\Delta U_{s,f}^{T-2000}$ ) as an example, the calculation for decomposing the effect of this factor can be presented as Eq. (6):

$$\Delta U_{s,f}^{T-2000} = (Emis_{s,f}^T - Emis_{s,f}^{2000}) / (\ln Emis_{s,f}^T - \ln Emis_{s,f}^{2000}) * \ln(U_{s,f}^T / U_{s,f}^{2000}) \quad (6)$$

Based on the inherent properties of each driving factor, and to facilitate comparison, the factors in Eqs. (2)–(4) are consolidated into four drivers in the following analysis. The improvement in emission efficiency ( $U$ ) is recognized as the effect of environmental control policies to reduce emission intensity. Shifts in energy consumption structure ( $F$ ) and energy intensity ( $I$ ) are jointly regarded as the effect of energy-climate policy. Adjustments in the economic structure ( $Y$ ) are considered as the effect of economic structure. Impacts of economic development ( $Q$ ) and demographic changes ( $P$ ) are collectively regarded as the effect of economic growth.

### Principal component analysis and Gaussian Mixture Model clustering

Based on the LMDI decomposition results, the principal component analysis (PCA) and Gaussian Mixture Model (GMM) clustering algorithm are further employed to investigate regional disparities in co-drivers of air pollutant and CO<sub>2</sub> emissions across China. Changes in SO<sub>2</sub>, NO<sub>x</sub>, primary PM<sub>2.5</sub>, and CO<sub>2</sub> emissions ( $\Delta Emis$  in Eq. (5)), as well as the relative contributions of their six drivers, are selected together as the clustering variables. However, the high dimensionality and complexity of the decomposition results make it challenging to directly perform clustering analysis. To address this, PCA is employed on a set of seven variables to extract principal components that capture the key effects of these drivers on emission patterns. PCA is a dimensionality reduction technique that simplifies complex datasets through a linear transformation of multiple variables<sup>88,89</sup>. The composite indicators generated from the linear transformation are referred to as “principal components”. Each principal component represents a linear combination of the original variables, and all principal components remain mutually uncorrelated<sup>90</sup>. The PCA process involves the following steps:

First, data standardization is performed by subtracting the mean and dividing by the standard deviation of each variable as follows:

$$X_{standardized} = (X - \mu) / \sigma \tag{7}$$

where  $X$  is the original data matrix,  $\mu$  is the mean vector of each variable,  $\sigma$  is the standard deviation of each variable, and  $X_{standardized}$  denotes the standardized data.

Then, the covariance matrix of the standardized data is calculated as:

$$Cov(X_{standardized}) = X_{standardized}^T X_{standardized} / (n - 1) \tag{8}$$

where  $n$  denotes the number of samples, and  $Cov(X_{standardized})$  represents the covariance matrix.

Third, the eigenvalue decomposition of the covariance matrix is performed to identify principal components as follows:

$$Cov(X_{standardized})v = \lambda v \tag{9}$$

where  $v$  and  $\lambda$  represent the eigenvectors (i.e., principal components) and corresponding eigenvalues, respectively.

Finally, the eigenvectors are sorted in descending order of their corresponding eigenvalues, and the number of principal components retained is typically determined based on a cumulative explained variance ratio exceeding 80%. The standardized data  $X_{standardized}$  is then projected onto the selected principal components to generate the reduced-dimensional dataset ( $X_{PCA}$ ) using Eq. (10):

$$X_{PCA} = X_{standardized} V_k \tag{10}$$

where  $V_k$  represents the matrix containing the first  $k$  eigenvectors.

In this study, provincial results of seven variables across different periods, sectors, and pollutant species were aggregated, followed by PCA to reduce the dimensionality of the dataset. Four principal components were retained, and the corresponding scores for each principal component were calculated at the provincial level. Combined with the subsequent clustering analysis, the spatial heterogeneity in pollution-carbon co-control characteristics in different provincial types can be identified.

As an unsupervised learning algorithm, GMM clustering has emerged as a widely used clustering method due to its ability to model complex data distributions and handle clusters with varying shapes and densities<sup>91,92</sup>. Unlike the K-means method, which assumes uniform spherical clusters, GMM clustering assigns data points probabilistically and identifies clusters with distinct covariance structures, allowing for more flexible and refined clustering<sup>93,94</sup>. GMM clustering aims to identify the underlying clusters in the dataset by estimating the parameters of Gaussian distributions through the Expectation-Maximization (EM) algorithm<sup>93</sup>. The clustering is

performed by maximizing the likelihood function of the dataset, where each data point is probabilistically assigned to a cluster based on the estimated parameters of the corresponding Gaussian distributions, which can be denoted as follows:

$$P(x) = \sum_{k=1}^K \pi_k f(x | \mu_k, \Sigma_k) \tag{11}$$

where  $K$  is the number of Gaussian clusters,  $\pi_k$  denotes the weight of the  $k$ -th Gaussian distribution, satisfying  $\sum_{k=1}^K \pi_k = 1$ ; and  $f(x | \mu_k, \Sigma_k)$  represents each Gaussian distribution with the average value  $\mu_k$  and covariance matrix  $\Sigma_k$ .

Based on the reduced-dimensional data from PCA, the four principal component scores for China’s 30 provinces served as input for GMM clustering. Due to the subjective nature of determining the number of clusters in the GMM algorithm, the Davies-Bouldin Index (DBI) is used to help identify the optimal cluster count and evaluate the quality of clustering results. Finally, seven provincial groups are identified through unsupervised clustering, ensuring that provinces in the same group share similar patterns in air pollutants and CO<sub>2</sub> co-control. PCA and GMM clustering analysis are performed using Python 3.9.

### Data availability

The Greenhouse Gas-Air Pollution Interactions and Synergies (GAINS) emission inventory is available from <https://gains.iiasa.ac.at/gains/EAN/index.login?logout=>. The socioeconomic statistics of the LMDI decomposition analysis can be accessed from <https://data.stats.gov.cn/easyquery.htm?cn=C01>.

### Code availability

The codes used for data processing and generating the results are available upon reasonable request from the corresponding author.

### Abbreviations

MEE	Ministry of Ecology and Environment of China
GAINS	Greenhouse Gas-Air Pollution Interactions and Synergies
LMDI	Logarithmic Mean Divisia Index
PCA	Principal component analysis
GMM	Gaussian Mixture Model
CEADs	Carbon Emission Accounts and Datasets
NBS	National Bureau of Statistics of China
FGD	flue-gas desulfurization
11 <sup>th</sup> FYP	11 <sup>th</sup> Five Year Plan
12 <sup>th</sup> FYP	12 <sup>th</sup> Five Year Plan
13 <sup>th</sup> FYP	13 <sup>th</sup> Five Year Plan
Phase I	Air Pollution Prevention and Control Action Plan
Phase II	Three-Year Action Plan for Winning the Blue Sky
Action Plan	Defense Battle
BTH	Beijing-Tianjin-Hebei Region
YRD	Yangtze River Delta

Received: 18 March 2025; Accepted: 10 June 2025;  
Published online: 01 July 2025

### References

- Geng, G. et al. Efficacy of China’s clean air actions to tackle PM2.5 pollution between 2013 and 2020. *Nat. Geosci.* <https://doi.org/10.1038/s41561-024-01540-z> (2024).
- Li, L. et al. Mitigation of China’s carbon neutrality to global warming. *Nat. Commun.* **13**, 5315 (2022).
- Xue, T. et al. New WHO global air quality guidelines help prevent premature deaths in China. *Natl. Sci. Rev.* **9**, nwac055 (2022).

4. Ministry of Ecology and Environment of the People's Republic of China. *National Ambient Air Quality Situation in 2023*, [https://www.mee.gov.cn/ywdt/xwfb/202401/t20240125\\_1064784.shtml](https://www.mee.gov.cn/ywdt/xwfb/202401/t20240125_1064784.shtml) (2023).
5. IEA. CO<sub>2</sub> emissions in 2023, <https://www.iea.org/reports/co2-emissions-in-2023> (2023).
6. Guo, Y. et al. Carbon mitigation and environmental co-benefits of a clean energy transition in China's industrial parks. *Environ. Sci. Technol.* **57**, 6494–6505 (2023).
7. Wu, Q. et al. Facility-level emissions and synergistic control of energy-related air pollutants and carbon dioxide in China. *Environ. Sci. Technol.* **57**, 4504–4512 (2023).
8. Li, S. et al. Integrated benefits of synergistically reducing air pollutants and carbon dioxide in China. *Environ. Sci. Technol.* <https://doi.org/10.1021/acs.est.4c00599> (2024).
9. Chen, Y. et al. Substantial differences in source contributions to carbon emissions and health damage necessitate balanced synergistic control plans in China. *Nat. Commun.* **15**, 5880 (2024).
10. Tong, D. et al. Targeted emission reductions from global super-polluting power plant units. *Nat. Sustain.* **1**, 59–68 (2018).
11. Wang, H. et al. Health benefits of on-road transportation pollution control programs in China. *Proc. Natl Acad. Sci. USA* **117**, 25370–25377 (2020).
12. Zhou, M. et al. Environmental benefits and household costs of clean heating options in northern China. *Nat. Sustain.* **5**, 329–338 (2021).
13. Sun, Y. et al. Air quality, health, and equity benefits of carbon neutrality and clean air pathways in China. *Environ. Sci. Technol.* <https://doi.org/10.1021/acs.est.3c10076> (2024).
14. Wu, K. et al. Mutual effects of CO<sub>2</sub> emission reduction and air pollution control policies in Beijing-Tianjin-Hebei region. *Front. Environ. Sci.* **10**, <https://doi.org/10.3389/fenvs.2022.1006142> (2022).
15. Jiang, J. et al. Two-tier synergic governance of greenhouse gas emissions and air pollution in China's Megacity, Shenzhen: impact evaluation and policy implication. *Environ. Sci. Technol.* **55**, 7225–7236 (2021).
16. Yang, Y., Xu, H., Yang, X., Zhang, Y. & Liu, T. Exploring synergistic efficiency of air pollution and carbon reduction and its influencing factors: insights from China. *Resources, Conserv. Recycling* **212**, <https://doi.org/10.1016/j.resconrec.2024.107973> (2025).
17. Shi, Q. et al. Co-benefits of CO<sub>2</sub> emission reduction from China's clean air actions between 2013–2020. *Nat. Commun.* **13**, 5061 (2022).
18. Tong, D. et al. Health co-benefits of climate change mitigation depend on strategic power plant retirements and pollution controls. *Nat. Clim. Change* **11**, 1077–1083 (2021).
19. Qin, Y. et al. Amplified positive effects on air quality, health, and renewable energy under China's carbon neutral target. *Nat. Geosci.* **17**, 411–418 (2024).
20. Huang, X., Srikrishnan, V., Lamontagne, J., Keller, K. & Peng, W. Effects of global climate mitigation on regional air quality and health. *Nat. Sustain.* <https://doi.org/10.1038/s41893-023-01133-5> (2023).
21. Wang, Y., Song, J., Yang, W., Dong, L. & Duan, H. Unveiling the driving mechanism of air pollutant emissions from thermal power generation in China: A provincial-level spatiotemporal analysis. *Resources Conserv. Recycling* **151**, <https://doi.org/10.1016/j.resconrec.2019.104447> (2019).
22. Zhang, Y. et al. Socioeconomic factors of PM<sub>2.5</sub> concentrations in 152 Chinese cities: decomposition analysis using LMDI. *J. Clean. Prod.* **218**, 96–107 (2019).
23. Sun, Y.-Y., Faturay, F., Lenzen, M., Gössling, S. & Higham, J. Drivers of global tourism carbon emissions. *Nat. Commun.* **15**, 10384 (2024).
24. Zhang, Q. et al. Drivers of improved PM<sub>2.5</sub> air quality in China from 2013 to 2017. *Proc. Natl Acad. Sci.* **116**, 24463–24469 (2019).
25. Geng, G. et al. Drivers of PM<sub>2.5</sub> air pollution deaths in China 2002–2017. *Nat. Geosci.* **14**, 645–650 (2021).
26. Wang, J. et al. The increasing role of synergistic effects in carbon mitigation and air quality improvement, and its associated health benefits in China. *Engineering* **20**, 103–111 (2023).
27. Li, Z., Wang, J. & Che, S. Synergistic effect of carbon trading scheme on carbon dioxide and atmospheric pollutants. *Sustainability* **13**, <https://doi.org/10.3390/su13105403> (2021).
28. Qi, Z. et al. Co-drivers of air pollutant and CO<sub>2</sub> emissions from on-road transportation in China 2010–2020. *Environ. Sci. Technol.* **57**, 20992–21004 (2023).
29. Wang, Y. et al. Analysis of synergistic drivers of CO<sub>2</sub> and NO<sub>x</sub> emissions from thermal power generating units in Beijing–Tianjin–Hebei region, 2010–2020. *Sustainability* **16**, <https://doi.org/10.3390/su16177554> (2024).
30. Yue, T. et al. Analysis of emission evolution and synergistic reduction effect of air pollutants and CO<sub>2</sub> from Chinese coal-fired power plants. *Atmos. Pollution Res.* **15**, <https://doi.org/10.1016/j.apr.2023.102001> (2024).
31. Zhao, H. et al. Heterogeneities in regional air pollutant emission mitigation across China during 2012–2020. *Earth Fut.* **12**, <https://doi.org/10.1029/2023ef004139> (2024).
32. Cheng, J. et al. A synergistic approach to air pollution control and carbon neutrality in China can avoid millions of premature deaths annually by 2060. *One Earth* **6**, 978–989 (2023).
33. People's Government of the People's Republic of China. *The CPC Central Committee's proposal on the formulation of the Eleventh Five-Year Plan*, [http://www.gov.cn/test/2008-08/20/content\\_1075373.htm](http://www.gov.cn/test/2008-08/20/content_1075373.htm) (2008).
34. The Central People's Government of the People's Republic of China. *Outline of the twelfth five-year plan for national economic and social development*, [https://www.gov.cn/test/2008-08/20/content\\_1075373.htm](https://www.gov.cn/test/2008-08/20/content_1075373.htm) (2011).
35. Wu, R. et al. Air quality and health benefits of China's emission control policies on coal-fired power plants during 2005–2020. *Environ. Res. Lett.* **14**, <https://doi.org/10.1088/1748-9326/ab3bae> (2019).
36. Wang, G. et al. Air pollutant emissions from coal-fired power plants in China over the past two decades. *Sci. Total Environ.* **741**, 140326 (2020).
37. National Bureau of Statistics of China. *China statistical yearbook 2011, 2016*, <http://www.stats.gov.cn/english/> (2011, 2016).
38. The Central People's Government of the People's Republic of China. *Action plan for the prevention and control of air pollutants*, [https://www.gov.cn/zwjgk/2013-09/12/content\\_2486773.htm](https://www.gov.cn/zwjgk/2013-09/12/content_2486773.htm) (2013).
39. Bo, X. et al. Effect of strengthened standards on Chinese ironmaking and steelmaking emissions. *Nat. Sustain.* **4**, 811–820 (2021).
40. The Central People's Government of the People's Republic of China. *Three-year action plan to win the battle against the blue sky*, [https://www.gov.cn/zhengce/content/2018-07/03/content\\_5303158.htm](https://www.gov.cn/zhengce/content/2018-07/03/content_5303158.htm) (2018).
41. Ma, T. et al. Costs and health benefits of the rural energy transition to carbon neutrality in China. *Nat. Commun.* **14**, 6101 (2023).
42. Zheng, B. et al. Changes in China's anthropogenic emissions and air quality during the COVID-19 pandemic in 2020. *Earth Syst. Sci. Data* **13**, 2895–2907 (2021).
43. Zhao, P., Li, Z., He, Z., Chen, Y. & Xiao, Z. Reducing the road freight emissions through integrated strategy in the port cities. *Nat. Commun.* **16**, 2563 (2025).
44. National Energy Administration. *China's energy conservation and emission reduction efforts during the 11th Five-Year Plan resulted in achievements in eight key areas*, [https://www.nea.gov.cn/2011-09/29/c\\_131166794.htm](https://www.nea.gov.cn/2011-09/29/c_131166794.htm) (2011).
45. The Central People's Government of the People's Republic of China. *Outline of the thirteenth five-year plan for national economic and social development*, [https://www.gov.cn/xinwen/2016-03/17/content\\_5054992.htm](https://www.gov.cn/xinwen/2016-03/17/content_5054992.htm) (2016).
46. Department of National Economic Accounting National Bureau of Statistics of China. *National input-output table of China 2005, 2010, 2015, 2020*, <http://www.stats.gov.cn/english/> (2005, 2010, 2015, 2020).

47. Zhu, B., Chen, G. & Wang, P. How does green fiscal policy promote the synergy of pollution mitigation and carbon reduction? Evidence from China. *Energy* **313**, <https://doi.org/10.1016/j.energy.2024.133700> (2024).
48. Liang, H., Bian, X. & Dong, L. Towards net zero carbon buildings: accounting the building embodied carbon and life cycle-based policy design for Greater Bay Area, China. *Geosci. Front.* **15**, <https://doi.org/10.1016/j.gsf.2023.101760> (2024).
49. National Bureau of Statistics of China. *China statistical yearbook 2001, 2021*, <http://www.stats.gov.cn/english/> (2001, 2021).
50. Zhang, W. X. et al. Rigorous regional air quality standards for substantial health benefits. *Earth Fut.* **11**, 13 (2023).
51. The Central People's Government of the People's Republic of China. *The state council's guidelines on supporting the transfer of industries to the Central and Western regions*, [https://www.gov.cn/zwgg/2010-09/06/content\\_1696516.htm](https://www.gov.cn/zwgg/2010-09/06/content_1696516.htm) (2010).
52. Zhang, C.-Y., Yu, B., Chen, J.-M. & Wei, Y.-M. Green transition pathways for cement industry in China. *Resources Conserv. Recycling* **166**, <https://doi.org/10.1016/j.resconrec.2020.105355> (2021).
53. P, M. et al. Energy savings, emission reductions, and health co-benefits of the green building movement. *J. Expo. Sci. Environ. Epidemiol.* **28**, 307–318 (2018).
54. Gao, X., Liu, N. & Hua, Y. Environmental Protection Tax Law on the synergy of pollution reduction and carbon reduction in China: Evidence from a panel data of 107 cities. *Sustain. Prod. Consum.* **33**, 425–437 (2022).
55. Hu, J. Synergistic effect of pollution reduction and carbon emission mitigation in the digital economy. *J. Environ. Manag.* **337**, 117755 (2023).
56. Tang, L. et al. Plant-level real-time monitoring data reveal substantial abatement potential of air pollution and CO<sub>2</sub> in China's cement sector. *One Earth* **5**, 892–906 (2022).
57. Zhang, S., Xie, Y., Sander, R., Yue, H. & Shu, Y. Potentials of energy efficiency improvement and energy–emission–health nexus in Jing-Jin-Ji's cement industry. *J. Cleaner Prod.* **278**, <https://doi.org/10.1016/j.jclepro.2020.123335> (2021).
58. The Central People's Government of the People's Republic of China. *Ministry of Industry and Information Technology and other eight departments on accelerating the transformation and upgrading of traditional manufacturing industry guidelines*, [https://www.gov.cn/zhengce/zhengceku/202312/content\\_6923270.htm](https://www.gov.cn/zhengce/zhengceku/202312/content_6923270.htm) (2023).
59. Liang, X. et al. Air quality and health benefits from fleet electrification in China. *Nat. Sustain.* **2**, 962–971 (2019).
60. Yuan, R. et al. Coordinated effects of energy transition on air pollution mitigation and CO<sub>2</sub> emission control in China. *Sci. Total Environ.* **841**, 156482 (2022).
61. The Central People's Government of the People's Republic of China. *Catalog of Encouraged Industries in Western Region*, [https://www.gov.cn/zhengce/zhengceku/2021-01/26/content\\_5582791.htm](https://www.gov.cn/zhengce/zhengceku/2021-01/26/content_5582791.htm) (2021).
62. China State Council. *Working guidance for carbon dioxide peaking and carbon neutrality in full and faithful implementation of the new development philosophy*, [http://english.www.gov.cn/policies/latestreleases/202110/25/content\\_WS61760047c6d0df57f98e3c21.html](http://english.www.gov.cn/policies/latestreleases/202110/25/content_WS61760047c6d0df57f98e3c21.html) (2021).
63. Wang, Y. et al. Accelerating the energy transition towards photovoltaic and wind in China. *Nature* **619**, 761 (2023).
64. Li, W. et al. Assessment of greenhouse gasses and air pollutant emissions embodied in cross-province electricity trade in China. *Resources Conserv. Recycling* **171**, <https://doi.org/10.1016/j.resconrec.2021.105623> (2021).
65. Zhang, Y., Zhao, Y., Gao, M., Bo, X. & Nielsen, C. P. Air quality and health benefits from ultra-low emission control policy indicated by continuous emission monitoring: a case study in the Yangtze River Delta region, China. *Atmos. Chem. Phys.* **21**, 6411–6430 (2021).
66. Cheng, J. et al. Pathways of China's PM<sub>2.5</sub> air quality 2015–2060 in the context of carbon neutrality. *Natl Sci. Rev.* **8**, nwab078 (2021).
67. Shi, X. et al. Air quality benefits of achieving carbon neutrality in China. *Sci. Total Environ.* **795**, 148784 (2021).
68. Li, Z. & Hanaoka, T. Plant-level mitigation strategies could enable carbon neutrality by 2060 and reduce non-CO<sub>2</sub> emissions in China's iron and steel sector. *One Earth* **5**, 932–943 (2022).
69. Yan, X. et al. Historical air pollutant emissions and future sustainable pathways of global cement plants. *Resources Conserv. Recycling* **211**, <https://doi.org/10.1016/j.resconrec.2024.107896> (2024).
70. Wang, P. et al. Location-specific co-benefits of carbon emissions reduction from coal-fired power plants in China. *Nat. Commun.* **12**, 6948 (2021).
71. Jiang, T., Zhang, R., Zhang, F., Shi, G. & Wang, C. Assessing provincial coal reliance for just low-carbon transition in China. *Environ. Impact Assess. Rev.* **102**, <https://doi.org/10.1016/j.eiar.2023.107198> (2023).
72. Amann, M. et al. Reducing global air pollution: the scope for further policy interventions. *Philos. Trans. R. Soc. A Math., Phys. Eng. Sci.* **378**, 20190331 (2020).
73. Klimont, Z. et al. Global anthropogenic emissions of particulate matter including black carbon. *Atmos. Chem. Phys.* **17**, 8681–8723 (2017).
74. National Bureau of Statistics of China. *China energy statistical yearbook 2020*, <http://www.stats.gov.cn/english/> (2020).
75. Cui, C. et al. Energy-related CO<sub>2</sub> emission accounts and datasets for 40 emerging economies in 2010–2019. *Earth Syst. Sci. Data* **15**, 1317–1328 (2023).
76. National Bureau of Statistics of China. *China price index statistical yearbook 2000–2020*, <http://www.stats.gov.cn/english/> (2000–2020).
77. Larsen, S. V., Kørnø, L. & Wejs, A. Mind the gap in SEA: an institutional perspective on why assessment of synergies amongst climate change mitigation, adaptation and other policy areas are missing. *Environ. Impact Assess. Rev.* **33**, 32–40 (2012).
78. Vigié, V. & Hallegatte, S. Trade-offs and synergies in urban climate policies. *Nat. Clim. Change* **2**, 334–337 (2012).
79. Yi, H., Zhao, L., Qian, Y., Zhou, L. & Yang, P. How to achieve synergy between carbon dioxide mitigation and air pollution control? Evidence from China. *Sustain. Cities Soc.* **78**, <https://doi.org/10.1016/j.scs.2021.103609> (2022).
80. von Schneidemesser, E. & Monks, P. S. Air quality and climate-synergies and trade-offs. *Environ. Sci. Process Impacts* **15**, 1315–1325 (2013).
81. Rana, E. A. K., Thwaites, R. I. K. & Luck, G. Trade-offs and synergies between carbon, forest diversity and forest products in Nepal community forests. *Environ. Conserv.* **44**, 5–13 (2016).
82. Shan, Y. L. et al. City-level emission peak and drivers in China. *Sci. Bull.* **67**, 1910–1920 (2022).
83. Liu, Y. et al. Heterogeneity of population exposure to particulate matter pollution and its socioeconomic driving mechanism in Shaanxi Province, China. *Environ. Pollut.* **363**, 125274 (2024).
84. Xu, S.-C., He, Z.-X. & Long, R.-Y. Factors that influence carbon emissions due to energy consumption in China: decomposition analysis using LMDI. *Appl. Energy* **127**, 182–193 (2014).
85. Ang, B. W. The LMDI approach to decomposition analysis: a practical guide. *Energy Policy* **33**, 867–871 (2005).
86. Ang, B., Zhang, F. & Choi, K. Factorizing changes in energy and environmental indicators through decomposition. *Energy* **23**, 489–495 (1998).
87. Ang, B. W. LMDI decomposition approach: a guide for implementation. *Energy Policy* **86**, 233–238 (2015).
88. Pearson, K. L. III On lines and planes of closest fit to systems of points in space. *Lond. Edinb. Dublin Philos. Mag. J. Sci.* **2**, 559–572 (1901).
89. Bro, R. & Smilde, A. K. Principal component analysis. *Anal. Methods* **6**, 2812–2831 (2014).
90. Greenacre, M. et al. Principal component analysis. *Nat. Rev. Methods Primers* **2**, <https://doi.org/10.1038/s43586-022-00184-w> (2022).

91. Ahmed, S. R. A., Al\_Barazanchi, I., Jaaz, Z. A. & Abdulshaheed, H. R. Clustering algorithms subjected to K-mean and Gaussian mixture model on multidimensional data sets. *Period. Eng. Nat. Sci.* **7**, 448–457 (2019).
92. Wang, S., Azzari, G. & Lobell, D. B. Crop type mapping without field-level labels: random forest transfer and unsupervised clustering techniques. *Remote Sens. Environ.* **222**, 303–317 (2019).
93. Andriyanov, N., Tashlinsky, A. & Dementiev, V. In *Intelligent systems and applications: proceedings of the 2020 intelligent systems conference (IntelliSys)*, 2. 437–448 (Springer, 2020).
94. Saxena, A. et al. A review of clustering techniques and developments. *Neurocomputing* **267**, 664–681 (2017).

## Acknowledgements

This work is supported by the National Key R&D Program of China (2023YFC3708600), the National Natural Science Foundation of China (42375191, 72243008), and the Joint Research Program for Ecological Conservation and High Quality Development of the Yellow River Basin (2022-YRUC-01-0406), and the Shuimu Tsinghua Scholar Program (2023SM027).

## Author contributions

W.C.: Writing - original draft, Visualization, Methodology, Investigation, Data curation. Y.Z.: Writing - review & editing, Validation, Supervision, Methodology, Data curation, Conceptualization. S.Z.: Writing - review & editing, Data curation, Methodology. Z.K.: Writing - review & editing, Data curation, Methodology. X.W.: Writing - review & editing, Supervision, Methodology, Data curation, Conceptualization. F.J.: Data curation. Z.Q.: Data curation. C.C.: Methodology. Y.F.: Methodology. Z.Z.: Writing - review & editing. H.Z.: Writing - review & editing. Y.L.: Writing - review & editing, Conceptualization. G.Y.: Writing - review & editing, Supervision, Methodology, Formal analysis, Conceptualization, Project administration.

## Competing interests

The authors declare no competing interests.

## Additional information

**Supplementary information** The online version contains supplementary material available at <https://doi.org/10.1038/s41612-025-01124-7>.

**Correspondence** and requests for materials should be addressed to Yixuan Zheng, Xian'en Wang or Gang Yan.

**Reprints and permissions information** is available at <http://www.nature.com/reprints>

**Publisher's note** Springer Nature remains neutral with regard to jurisdictional claims in published maps and institutional affiliations.

**Open Access** This article is licensed under a Creative Commons Attribution-NonCommercial-NoDerivatives 4.0 International License, which permits any non-commercial use, sharing, distribution and reproduction in any medium or format, as long as you give appropriate credit to the original author(s) and the source, provide a link to the Creative Commons licence, and indicate if you modified the licensed material. You do not have permission under this licence to share adapted material derived from this article or parts of it. The images or other third party material in this article are included in the article's Creative Commons licence, unless indicated otherwise in a credit line to the material. If material is not included in the article's Creative Commons licence and your intended use is not permitted by statutory regulation or exceeds the permitted use, you will need to obtain permission directly from the copyright holder. To view a copy of this licence, visit <http://creativecommons.org/licenses/by-nc-nd/4.0/>.

© The Author(s) 2025